



HAL
open science

Indigenous and exogenous organics and surface–atmosphere cycling inferred from carbon and oxygen isotopes at Gale crater

H. B. Franz, P. R. Mahaffy, C. R. Webster, G. J. Flesch, E. Raaen, Caroline Freissinet, S. K. Atreya, C. H. House, A. C. Mcadam, C. A. Knudson, et al.

► **To cite this version:**

H. B. Franz, P. R. Mahaffy, C. R. Webster, G. J. Flesch, E. Raaen, et al.. Indigenous and exogenous organics and surface–atmosphere cycling inferred from carbon and oxygen isotopes at Gale crater. *Nature Astronomy*, 2020, 4, pp.526-532. 10.1038/s41550-019-0990-x . insu-02538419

HAL Id: insu-02538419

<https://insu.hal.science/insu-02538419>

Submitted on 18 Dec 2020

HAL is a multi-disciplinary open access archive for the deposit and dissemination of scientific research documents, whether they are published or not. The documents may come from teaching and research institutions in France or abroad, or from public or private research centers.

L'archive ouverte pluridisciplinaire **HAL**, est destinée au dépôt et à la diffusion de documents scientifiques de niveau recherche, publiés ou non, émanant des établissements d'enseignement et de recherche français ou étrangers, des laboratoires publics ou privés.

Indigenous and exogenous organics and surface–atmosphere cycling inferred from carbon and oxygen isotopes at Gale crater

H. B. Franz^{1*}, P. R. Mahaffy¹, C. R. Webster², G. J. Flesch², E. Raaen¹, C. Freissinet³, S. K. Atreya⁴, C. H. House⁵, A. C. McAdam¹, C. A. Knudson^{1,6}, P. D. Archer Jr.^{7,8}, J. C. Stern¹, A. Steele⁹, B. Sutter^{7,8}, J. L. Eigenbrode¹⁰, D. P. Glavin¹⁰, J. M. T. Lewis^{1,10}, C. A. Malespin¹, M. Millan^{1,11}, D. W. Ming⁷, R. Navarro-González¹² and R. E. Summons¹³

Since landing at Gale crater, Mars, in August 2012, the Curiosity rover has searched for evidence of past habitability, such as organic compounds, which have proved elusive to previous missions. We report results from pyrolysis experiments by Curiosity's Sample Analysis at Mars (SAM) instrument, focusing on the isotopic compositions of evolved CO₂ and O₂, which provide clues to the identities and origins of carbon- and oxygen-bearing phases in surface materials. We find that O₂ is enriched in ¹⁸O (δ¹⁸O about 40‰). Its behaviour reflects the presence of oxochlorine compounds at the Martian surface, common to aeolian and sedimentary deposits. Peak temperatures and isotope ratios (δ¹⁸O from −61 ± 4‰ to 64 ± 7‰; δ¹³C from −25 ± 20‰ to 56 ± 11‰) of evolved CO₂ indicate the presence of carbon in multiple phases. We suggest that some organic compounds reflect exogenous input from meteorites and interplanetary dust, while others could derive from in situ formation processes on Mars, such as abiotic photosynthesis or electrochemical reduction of CO₂. The observed carbonate abundances could reflect a sink for about 425–640 millibar of atmospheric CO₂, while an additional 100–170 millibar could be stored in oxalates formed at the surface. In addition, oxygen isotope ratios of putative carbonates suggest the possibility of widespread cryogenic carbonate formation during a previous era.

Because the climate of Mars may have been more compatible with life in the ancient past, a key focus of Mars exploration has involved the search for organic compounds that could have supported an ancient Martian biosphere. Curiosity's SAM instrument, which studies volatile compounds in scooped and drilled samples from the Martian surface, has detected several lines of evidence for organic carbon in Gale crater, including ion fragments typical of aliphatic and aromatic hydrocarbons as well as chlorobenzene, dichloroalkanes and thiophenes^{1,2}. Over geologic time, organic compounds may be transformed to metastable intermediates such as oxalate and acetate that accumulate at the surface and are detectable by SAM^{3,4}. The abundance of carbon associated with these compounds in SAM data is substantially greater than that estimated for exogenous organic matter, implying in situ formation mechanisms (see Supplementary Information). In addition to organic compounds, SAM has detected potential evidence for carbonate in some samples⁵, which could reflect a surface sink for CO₂ from a thicker ancient atmosphere⁶.

SAM carries two instruments—a quadrupole mass spectrometer (QMS) and a tunable laser spectrometer (TLS)—that measure isotope ratios in Martian volatile compounds. Measurements of Martian atmospheric CO₂ by both instruments have revealed

isotopic enrichment in carbon and oxygen, with ¹³C/¹²C of atmospheric carbon elevated by about 60‰ or more compared to carbon from the Martian mantle^{7,8}. The isotopic composition of CO₂ evolved from samples as they are heated can offer insights into carbon and oxygen sources and communication between atmospheric and surface volatile reservoirs.

Samples and analytical results

The samples discussed here represent both aeolian deposits and sedimentary rocks within Gale crater, investigated during an approximately 19.5-km-long traverse from November 2012 to November 2017 that climbed approximately 375 m in elevation. Ten samples acquired by Curiosity's drill and three obtained by scooping of aeolian deposits yielded robust measurements of CO₂ isotopic composition. One drilled sample and one aeolian sample also yielded isotopic analyses of O₂. The geological context for these samples, identified in Fig. 1, is described in the Supplementary Information.

Carbon and oxygen isotope ratios (δ¹³C and δ¹⁸O) for evolved CO₂ and O₂ as measured by the QMS are reported in Supplementary Tables 1 and 2, while CO₂ and O₂ release profiles are shown in Extended Data Fig. 1. Uncertainties (±1σ) represent the standard error of the mean for isotope ratios near peak maximum.

¹NASA Goddard Space Flight Center, Greenbelt, MD, USA. ²Jet Propulsion Laboratory, California Institute of Technology, Pasadena, CA, USA. ³LATMOS-IPSL/CNRS, University of Versailles St Quentin, Guyancourt, France. ⁴Department of Climate and Space Sciences, University of Michigan, Ann Arbor, MI, USA. ⁵Department of Geosciences, Pennsylvania State University, University Park, PA, USA. ⁶Department of Astronomy, University of Maryland, College Park, MD, USA. ⁷NASA Johnson Space Center, Houston, TX, USA. ⁸Jacobs Technology, Houston, TX, USA. ⁹Geophysical Laboratory, Carnegie Institute of Washington, Washington, DC, USA. ¹⁰Universities Space Research Association, Columbia, MD, USA. ¹¹Department of Biology, STIA, Georgetown University, Washington, DC, USA. ¹²Instituto de Ciencias Nucleares, Universidad Nacional Autónoma de México, Ciudad Universitaria, México City, México. ¹³Department of Earth, Atmospheric and Planetary Sciences, Massachusetts Institute of Technology, Cambridge, MA, USA.

*e-mail: heather.b.franz@nasa.gov

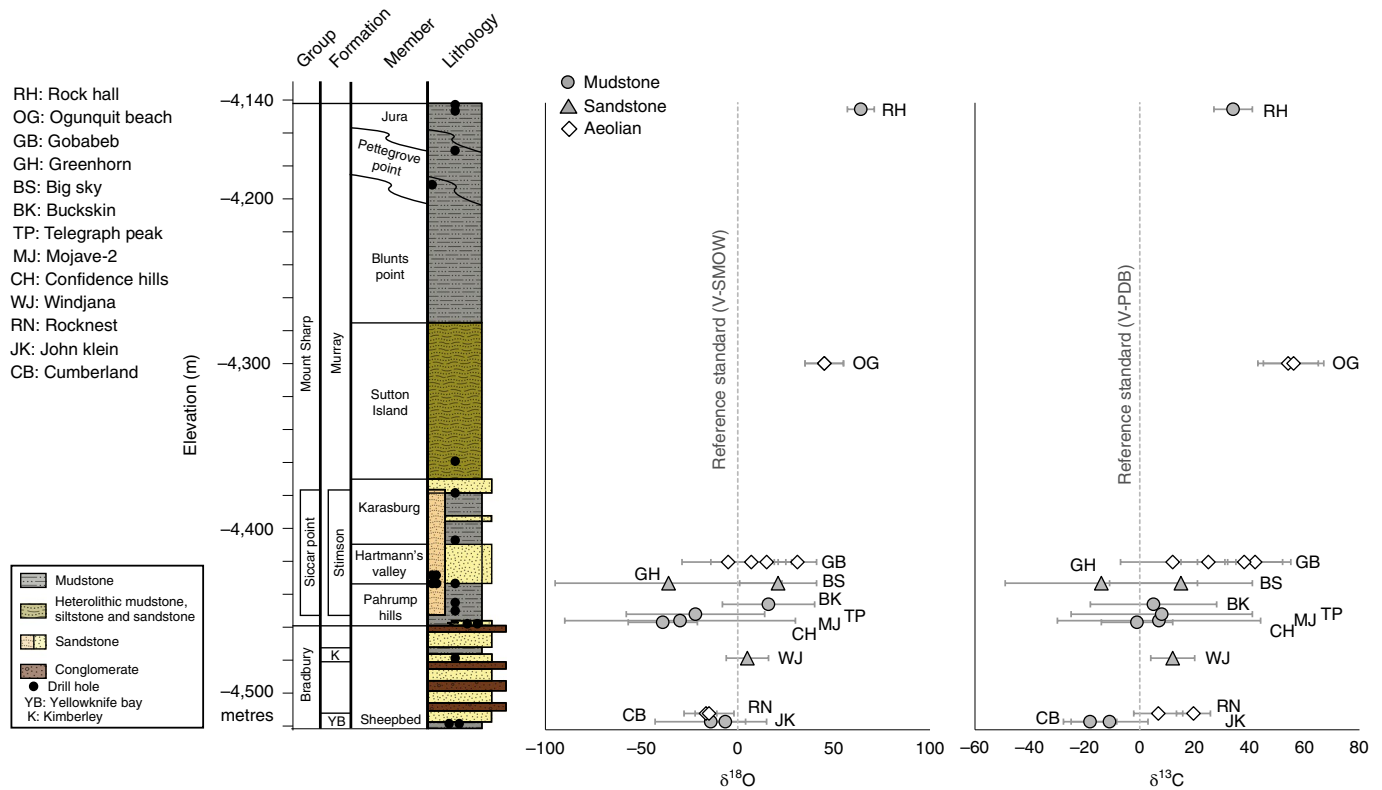


Fig. 1 | CO₂ isotopic composition displayed in stratigraphic context. The y-axis gives the elevation from the reference areoid, shown here as a proxy for the thickness of rock observed. Samples were acquired from various geologic members, which are subunits of formations, the fundamental lithostratigraphic units. Formations related by lithology, lateral continuity or other similarities may be organized into groups as shown. The stratigraphic column was prepared by the MSL Sedimentology and Stratigraphy Working Group. Vienna Standard Mean Ocean Water (V-SMOW) and Vienna Pee Dee Belemnite (V-PDB) are the reference standards for the oxygen and carbon isotopes, respectively⁵¹. The error bars are 1σ .

Supplementary Table 1 also includes isotope data obtained with the TLS for a subset of samples, with the TLS temperature cut in column 4. ‘Temperature cut’ refers to a range of temperatures as the oven is ramping during which a portion of the gas stream is collected by the TLS for analysis. The CO₂ isotopic composition of each sample is plotted in stratigraphic context in Fig. 1. CO₂ shows carbon isotope ratios spanning the range between compositions similar to those of Martian mantle carbon and atmospheric CO₂. Oxygen isotope ratios of evolved CO₂ show a similar range of fractionation with respect to the terrestrial oxygen isotope standard, and O₂ released from oxychlorine compounds has ¹⁸O enrichment approaching that of atmospheric CO₂. Weighted averages for $\delta^{18}\text{O}$ of O₂ evolved from oxychlorine compounds in aeolian deposits at Rocknest ($40 \pm 3\text{‰}$) and the Cumberland mudstone ($41 \pm 4\text{‰}$) were in close agreement. These results indicate activity of geochemical cycling on Mars that has facilitated transfer between surface and atmospheric reservoirs of carbon and oxygen.

Potential sources of evolved CO₂

Potential known sources of CO₂ released during SAM experiments include instrument background from *N*-methyl-*N*-(tert-butyl)dimethylsilyl)-trifluoroacetamide (MTBSTFA) products ($\delta^{13}\text{C}$ of -35‰), adsorbed atmospheric CO₂ ($\delta^{18}\text{O}$ about 50‰ and $\delta^{13}\text{C}$ about 45‰ ⁷), magmatic carbon ($\delta^{13}\text{C}$ of $-19 \pm 4.5\text{‰}$ ⁸), carbonates, and exogenous carbon from meteorites and interplanetary dust. As discussed in the Methods, combustion of instrument background components should primarily contribute to CO₂ evolved below around 150°C , well below the major CO₂ releases, and corrections for isobaric interferences from known MTBSTFA products minimize

effects on computed isotope ratios. Adsorbed atmospheric CO₂ evolves for a similar temperature range and should also have minimal effects on isotopic compositions obtained for most samples. However, results for CO₂ peaks below 200°C are reported in the Supplementary Information but are not included in the main discussion because they are likely to include indeterminate contributions from these sources.

A graph of $\delta^{18}\text{O}$ and $\delta^{13}\text{C}$ measured by SAM versus CO₂ peak temperature (Fig. 2) suggests that the data fall into three general groups: (I) a low-temperature group (Yellowknife Bay) with depletions in both ¹⁸O and ¹³C; (II) a mid-temperature group (Rocknest, Murray formation, and Stimson formation) with depletions in ¹⁸O (except at Big Sky) but some enrichment in ¹³C; and (III) a high-temperature group (Bagnold dunes) enriched in both ¹⁸O and ¹³C. These relationships suggest differences in sources of carbon and oxygen among the groups. Referring to Extended Data Fig. 2, CO₂ peaks at low and medium temperatures suggest evolution from salts of organic acids or oxalates, while high-temperature peaks are consistent with evolution from Fe or Mg carbonates. The Rock Hall sample was unique in evolving isotopically enriched CO₂ at low temperature, with possible reasons offered below. Results for individual samples are discussed in the Supplementary Information.

Potential isotopic fractionation mechanisms

Fractionation by atmospheric escape. Collective isotopic data for Martian atmospheric gases suggest that Mars lost most of its primordial atmosphere owing to hydrodynamic escape prior to about 4.3 billion years ago⁹ and that evolution of the atmosphere since that time has been driven by a combination of replenishment by volcanic

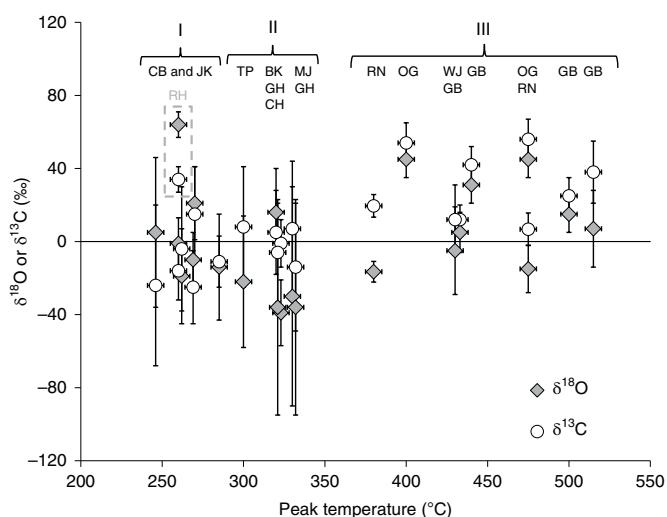


Fig. 2 | CO₂ isotopic composition ($\delta^{18}\text{O}$ and $\delta^{13}\text{C}$) versus associated evolved gas analysis (EGA) sample peak temperature. Brackets denote general sample groupings (I–III) as discussed in the main text. Sample abbreviations are given in Fig. 1. The Rock Hall (RH) sample was unique in evolving isotopically enriched CO₂ at low temperature and thus does not fit with the Yellowknife Bay samples in group I. The error bars are 1 σ .

outgassing and loss by ongoing escape to space^{7,10–12}, formation of carbonates and possibly other minerals at the surface^{6,13–17}, and sequestration in various regolith ice deposits^{9,18–22}. The continuous loss of gases from the exosphere of Mars to space, facilitated by the absence of a planetary magnetic field²³, favours the loss of isotopically light species and leaves the remaining atmosphere enriched in heavy isotopes¹⁸. In the absence of exchange with surface reservoirs, operation of this process over billions of years would generate gradually increasing values of $\delta^{13}\text{C}$ and $\delta^{18}\text{O}$ in atmospheric gases. Although the exact trajectory of $\delta^{13}\text{C}$ and $\delta^{18}\text{O}$ through history is uncertain, outgassing, mineral and ice formation, and isotopic exchange with surface reservoirs have also clearly influenced the isotopic composition of the modern atmosphere. We broadly assume that the net $\delta^{13}\text{C}$ and $\delta^{18}\text{O}$ of Martian atmospheric CO₂, O₂ and water have risen over geologic time, such that the modern composition is more isotopically enriched than the ancient composition. The net fractionation due to atmospheric loss throughout the history of Mars is greater than fractionations caused by other processes that we discuss.

Formation of secondary carbonates. Carbonates have been proposed as a sink for atmospheric CO₂, and limited evidence for carbonate minerals has been detected at Gale crater by Curiosity's Chemistry and Mineralogy (CheMin) instrument²⁴ and globally in thermal emission spectra by orbiting spacecraft²⁵. The ¹³C enrichment observed by SAM in aeolian samples (around 7–56‰), which evolved CO₂ at temperatures consistent with siderite, is within the range of that observed in most carbonates in Martian meteorites (about 7–65‰)^{26,27}. Most studies reporting ¹³C-enriched carbonates have concluded that they formed at low temperatures from fluids influenced by an atmosphere enriched in ¹³C and ¹⁸O through escape processes. For reference, magnesite or siderite forming in isotopic equilibrium with the current atmosphere at 25°C would have $\delta^{13}\text{C}$ of 50–60‰ and would be about 3‰ higher at 0°C (ref. 28). The observed values of $\delta^{13}\text{C}$ could be achieved by carbonate precipitation from a reservoir depleted in ¹³C relative to the modern atmosphere—for example, fluid from which carbonates had already precipitated—or by carbonate formation earlier in Mars' history, when atmospheric CO₂ was less isotopically depleted. Earlier

episodes of carbonate formation probably would have occurred during the Noachian period, before extensive volcanism produced aerosols that acidified surface waters²⁹. Minor contributions to high-temperature CO₂ peaks from combustion of ¹³C-depleted organic compounds would also lower $\delta^{13}\text{C}$.

The ¹⁸O enrichment observed in CO₂ evolved from samples of the Bagnold dunes ($\delta^{18}\text{O}$ about –5‰ to 43‰) is also similar to that in meteorite carbonates ($\delta^{18}\text{O}$ ~1‰ to 32‰)³⁰. The fractionation factor for siderite precipitation at 25°C predicts an ¹⁸O enrichment of around 10‰ with respect to CO₂ (ref. 31). Carbonates formed in equilibrium with the modern Martian atmosphere thus would have $\delta^{18}\text{O}$ above that observed in meteorites and some Gobabeb peaks, suggesting that the fluids from which at least a portion of the carbonates at Gobabeb formed either had been buffered by silicates or had been isotopically fractionated by freezing or mineral precipitation. On Earth, an effective fractionation constant of 2‰ to 3‰ between sea water and ice preferentially partitions ¹⁸O into the solid phase, leaving the remaining sea water depleted in ¹⁸O (ref. 32). Carbonates and sulfates substantially depleted in ¹⁸O compared to sea water are common in isolated Antarctic basins, producing progressively depleted brines through Rayleigh distillation during gradual freezing³³. Morphological observations suggest that some areas of Gale crater may have hosted lakes partially or totally covered by ice during the Hesperian period or later³⁴. Alternatively, ¹⁸O-depleted carbonates could precipitate from a body of water already fractionated owing to prior mineral formation. At 25°C, minerals typically carry ¹⁸O enrichments of up to about 40‰ compared to the water from which they precipitate³⁵, leaving the remaining water depleted in ¹⁸O.

Oxidation of carbon-bearing phases. The Martian surface is exposed to reduced carbon delivered both from the Martian mantle through volcanism and from impacting meteorites. Studies of Martian meteorites have revealed organic matter with $\delta^{13}\text{C}$ of –13‰ to 33‰, while impacting meteorites of chondritic composition could deliver organics with $\delta^{13}\text{C}$ from about –35‰ to 50‰ (see Supplementary Information)^{8,36}. Overlap of O₂ and CO₂ evolution during SAM analyses of Gale crater samples has prompted suggestions that the CO₂ may reflect combustion of organic carbon during pyrolysis. Similar isotopic compositions in O₂ released from the Rocknest and Cumberland samples support a potentially widespread occurrence of an oxychlorine component, as proposed on the basis of the common relationship between nitrate and perchlorate abundances observed by SAM in samples of all types³⁷. The average $\delta^{18}\text{O}$ (about 40‰, Supplementary Table 2) of the O₂ shows substantial enrichment in ¹⁸O compared to Martian silicates, suggesting the influence of escape processes that are evident in atmospheric CO₂, and even greater ¹⁸O enrichment compared to the CO₂ released from the Rocknest, Yellowknife Bay and Murray formation samples. Combustion would not be expected to introduce large fractionation in oxygen isotopes between O₂ and product CO₂, suggesting that while combustion of reduced organic matter by O₂ from oxychlorine may have occurred, it was not the dominant source of CO₂ evolved from most samples.

Another possibility is that CO₂ evolved from mudstones represents carbon from various source materials oxidized at the Martian surface rather than in the pyrolysis oven. Several species of oxidants potentially threaten the stability of organic matter on Mars, including perchlorate and other oxychlorine compounds, hydrogen peroxide and superoxide and hydroxyl ($\cdot\text{OH}$) radicals³⁸. The long-prevailing perspective is that the presence of strong oxidants, as well as ultraviolet radiation, would restrict the residence time of organic matter at the Martian surface and completely prevent its detection by in situ explorers. However, SAM observations interpreted as evidence for organic compounds preserved in minerals suggest that this may not be the case^{1,2}. In addition, Benner et al.³ identified

reaction mechanisms by which $\cdot\text{OH}$ attack on organic compounds typical of carbonaceous chondrites would form metastable intermediates, such as mellitic acid, oxalates, and acetates, that could have accumulated over geologic time to levels detectable by SAM. Applin et al.⁴ reported that oxalate minerals, which their experimental results imply would be as stable to ultraviolet radiation at the surface as sulfates and carbonates, would be particularly amenable to accumulation at the surface.

Most studies of organic compound degradation by $\cdot\text{OH}$ radicals have found associated fractionations of carbon isotopes to be $\leq 10\text{‰}$ (ref. ³⁹), although larger fractionations of up to about 25‰ have been observed in reactions of alkene double bonds with $\cdot\text{OH}$ (ref. ⁴⁰). Even with the potential for some fractionation during oxidation, the values of $\delta^{13}\text{C}$ measured by SAM fall within the range observed in meteorites of both Martian and non-Martian origin.

Although some precursor compounds in meteoritic organics contain oxygen, the $\delta^{18}\text{O}$ of CO_2 released through decarboxylation of oxidative products would probably be dominated by the composition of the oxidant as well as fractionation during oxidation. We assume that kinetic isotope effects during oxidation might introduce some degree of ^{18}O depletion in products compared to the oxidant, which could explain the ^{18}O depletions in CO_2 evolved from samples in groups I and II of Fig. 2. Depending on the water-to- CO_2 and water-to-rock ratios, water within a lake at Gale crater could be expected to have $\delta^{18}\text{O}$ of about 5–10‰ (ref. ³¹), requiring ^{18}O depletion of 10–45‰ during aqueous oxidation reactions to reach the compositions observed in mudstones. A more depleted starting composition for water could be obtained through fractionation due to partial freezing or previous mineral precipitation, as discussed above.

Another scenario would involve oxidation of organic matter through surface reactions with adsorbed $\cdot\text{OH}$. Owing to low atmospheric pressure, ultraviolet radiation penetrates the entire Martian atmospheric column, allowing the operation of photochemical processes near the surface that on Earth occur only in the stratosphere. The dominant pathways for formation of $\cdot\text{OH}$ in the Martian atmosphere are the reaction of HO_2 with O atoms and H_2O_2 photolysis, both of which are ultimately governed by H_2O photolysis⁴¹. Photolysis of ozone and CO_2 can generate ^{18}O -depleted O atoms, and photocatalysed or electrochemical reduction of water could favour production of $\cdot\text{OH}$ radicals with light oxygen, which could in turn generate ^{18}O -depleted products upon oxidation of organic matter and augment ^{18}O depletion due to kinetic isotope effects during oxidation (see Supplementary Information).

In situ formation of organic compounds. From the evolved CO_2 abundances compared to exogenous input, it seems likely that some organic material or oxalates at Gale crater formed in situ on Mars. Fischer–Tropsch-type synthesis may form a variety of hydrocarbons abiotically in terrestrial and extraterrestrial environments. Laboratory studies have shown the products of Fischer–Tropsch-type synthesis to include aliphatic hydrocarbons and amino acids, which may be oxidized to more stable compounds at the surface, as just discussed (see Supplementary Information). Organics may also be formed by other mechanisms, potentially even in the modern Martian environment. Numerous organic compounds may be produced through photolytic or catalytic reactions driven by light at ultraviolet and visible wavelengths, including photolysis of water-and-gas mixtures and abiotic photosynthesis, in which reduction of CO_2 is photocatalysed at semiconductor mineral surfaces (see Supplementary Information). Similar reactions may occur during electrochemical CO_2 reduction, powered by non-solar energy sources⁴². In laboratory studies, products of these processes have included carboxylated compounds such as formic acid, formaldehyde and oxalate as well as methane and alcohols. Ultraviolet irradiation of siderite in the presence of water has also been shown to yield

formate, formaldehyde and their derivatives (see Supplementary Information). Many of the compounds produced by the above processes may be oxidized to accumulate as oxalate minerals that would decarboxylate during pyrolysis^{3,4}.

During vapour-phase reactions at mineral surfaces, initial adsorption would probably introduce only small isotopic fractionations ($< 2\text{‰}$)⁴³. Although biological photosynthesis is complicated by the involvement of enzymes through multiple steps, at present it offers our best analogue for understanding potential fractionations during photocatalysed reduction of CO_2 at mineral surfaces. Assuming similar kinetic isotope effects during the abiotic process predicts products with ^{13}C depletions of up to 20–30‰ compared to atmospheric CO_2 .

The oxygen isotopic compositions of plants are not ideal analogues for abiotic reduction products, but laboratory experiments investigating ultraviolet photocatalytic reduction of CO_2 to formic acid showed that water functioned as the electron donor to produce oxygen and organic molecules, similar to plant photosynthesis. If the fractionation associated with this process is similar to that observed in oxidation of water by transition metal ions, which evolved oxygen depleted in ^{18}O by about 29‰ compared to water, then with an average atmospheric $\delta^{18}\text{O}$ of around 50‰, the oxygen isotopic composition of CO_2 reduction products could be expected to have $\delta^{18}\text{O}$ of about 10–20‰ (see Supplementary Information). Both $\delta^{13}\text{C}$ and $\delta^{18}\text{O}$ values predicted by analogy to terrestrial photosynthetic processes fall within the range of values measured by SAM, supporting abiotic photosynthesis as a potential source of compounds evolving CO_2 at low and medium temperatures.

Implications for the Martian carbon cycle. Carbon-bearing phases detected in Gale crater sediments probably reflect multiple sources and various geochemical processes (Fig. 3), which are relevant to understanding the history of Mars' climate and habitability. SAM observations of CO_2 evolved from aeolian deposits at the Bagnold dunes with temperatures and isotope ratios consistent with possible siderite support the formation of carbonates as a surface sink for CO_2 . The Rock Hall mudstone sample, with CO_2 of similar isotopic composition to that from Ogunquit Beach and Gobabeb, was unique in evolving CO_2 at a peak temperature of about 260°C but enriched in both ^{13}C and ^{18}O and also containing akaganeite at several weight per cent (see Supplementary Information). Laboratory studies have shown that carbonates may evolve CO_2 at lower-than-normal temperatures through reaction with HCl released from akaganeite or oxychlorine compounds, also evident at Rock Hall. It is possible that CO_2 evolved from siderite at Rock Hall by this mechanism (see Supplementary Information). If so, carbonate at Rock Hall may reflect a local source for some of that observed at nearby dunes. Overlap in isotopic composition between the two peaks evolved from each Bagnold dune sample would be consistent with two size fractions of Fe-carbonate, a dust component represented by the peak temperature range of about 400–425°C and larger grains represented by the peak temperature range of about 475–525°C. It is notable, however, that the peak temperatures and isotopic composition were similar between the coarse and fine size fractions of the Gobabeb sample, suggesting a common origin for carbonate in these fractions. Given that the larger grains probably represent local rather than global sediments, assignment of the dust fraction to a global component would imply that formation of carbonate occurred by a similar mechanism and under similar conditions at a large scale.

Abundances of CO_2 released from the Gobabeb 1 and Ogunquit Beach 3 samples were equivalent to approximately 2.1 wt% and 1.4 wt% siderite, respectively. Following the calculations of Bridges et al.⁴⁴, these values would indicate a sink for around 425–640 mb of atmospheric CO_2 , if the siderite inferred to reside in these samples represents a global component⁴⁴. The isotopic compositions of CO_2

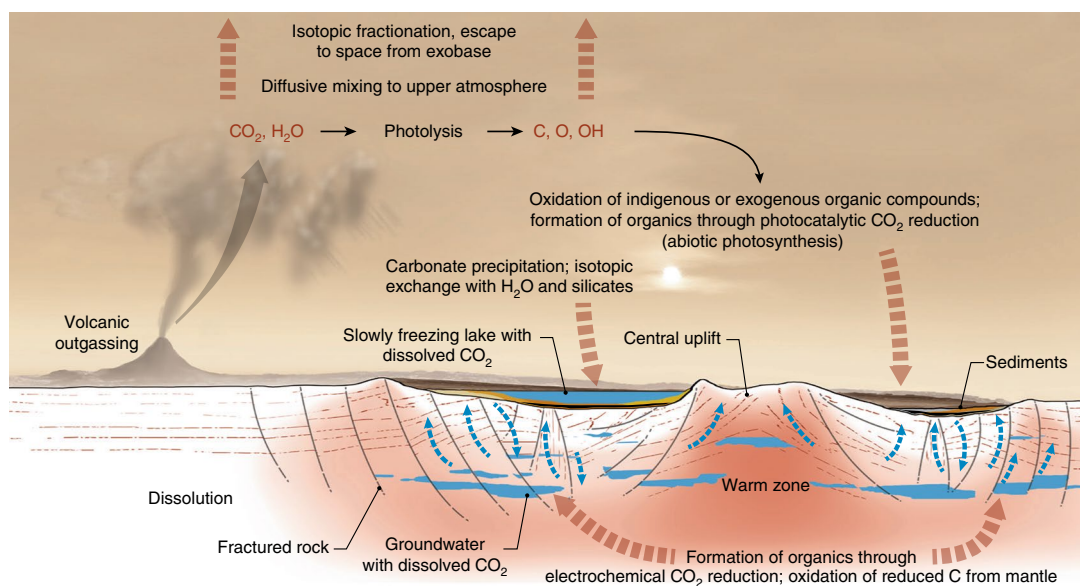


Fig. 3 | Sketch displaying major processes and environments that affected the isotopic composition of carbon and oxygen in Gale crater samples.

The details and relevance of each process are discussed in the text. Escape of CO_2 to space is an ongoing process that has gradually enriched the atmosphere in heavy isotopes over time. Fractionation due to other processes depicted in the figure is generally overprinted on the signature introduced by atmospheric escape. The blue arrows indicate circulation of ground water, whereas the brown arrows indicate reactions or transport of carbon- and oxygen-bearing phases.

evolved from Gobabeb and Ogunquit Beach, showing enrichments in both ^{18}O and ^{13}C , suggest the influence of atmospheric CO_2 fractionated by escape of light isotopes to space. However, the values of $\delta^{18}\text{O}$ and $\delta^{13}\text{C}$ for these samples are largely below those expected for formation of carbonate at equilibrium with the modern Martian atmosphere. This suggests either that the siderite formed predominantly during the Noachian period, when atmospheric CO_2 was less enriched in heavy isotopes than it is at present, and reflects a source region external to Gale crater, or that it precipitated from fluids isotopically fractionated with respect to the modern atmosphere, such as through partial freezing. If precipitation of carbonates from partially frozen reservoirs were widespread during a previous phase of history, then cryogenic carbonates could comprise a substantial fraction of carbonate inferred to reside in a global dust component. Isotopic analyses of carbonates in aeolian deposits at other sites across Mars are needed to determine whether the composition observed at Gale crater is likely to reflect locally or globally sourced material.

The evolution of CO_2 from all samples at temperatures consistent with various types of oxalate minerals could also reflect a sink for atmospheric CO_2 through abiotic photosynthesis. The variability in isotopic composition among the peaks of groups I and II (Fig. 2) suggests that probably only a subset of CO_2 peaks potentially derived from oxalate could reflect formation from atmospheric CO_2 . Because the isotopic fractionation and product yields associated with abiotic photosynthesis are at present unknown and may vary depending on the specific catalysts involved, we cannot be certain which samples may preserve evidence of this process or how much atmospheric CO_2 may be stored in oxalates within the regolith, but abundances of CO_2 from sandstones (Big Sky and Greenhorn) with isotope ratios closest to those predicted by analogy to plant photosynthesis suggest that if this component were globally distributed, it could store an additional 100–170 mb or so of atmospheric CO_2 . Given that this component was not detected in every sample by SAM, some oxalate could reflect oxidized organic compounds and some could have already degraded, this range represents an upper limit based on current inventory.

In addition to sequestering CO_2 , abiotic photosynthesis or electrochemical CO_2 reduction could yield organic matter of value to

chemotrophic organisms, by analogy to terrestrial environments. Electrochemical reduction of CO_2 during late-stage igneous or hydrothermal processes has been suggested as a potential source of organic carbon phases in maskelynite inclusions of the Tissint shergottite⁸. SAM has observed ^{34}S -depleted SO_2 in some mudstones of Yellowknife Bay and the Murray formation, interpreted to reflect Fe-sulfides derived from a hydrothermal system beneath Gale crater⁴⁵ that could also have delivered carbon-bearing compounds to overlying sediments. These compounds, as well as exogenous organic matter from meteorites and interplanetary dust, could contribute to the carbon inventory observed by SAM and to the potential habitability of Mars³.

It is feasible that both abiotic photosynthesis and delivery of exogenous material are ongoing on modern Mars, actively replenishing the surface with small quantities of organic compounds. Abiotic photosynthesis could also yield small amounts of methane and contribute to the variability in background methane detected by TLS (see Supplementary Information)⁴⁶. Although the Martian surface is currently inhospitable to Earth-like life, operation of these processes during earlier, more clement periods of Mars' history could have generated compounds useful to support a biosphere. If biological compounds were indeed present, surface/subsurface fluid exchange^{27,45} could have transferred these compounds to better-protected habitats and facilitated their preservation.

Methods

SAM EGA. SAM can analyse solid Martian samples obtained by drilling into rocks or scooping surface fines. Powdered samples, each with mass ~45 mg to ~135 mg, are passed through one of two sieves, either 150 μm or 1 mm, before loading into a quartz sample cup. All but one (Gobabeb 2, or "GB2") of the samples analysed by SAM to date have utilized the 150- μm sieve. The GB2 sample was processed through a 1-mm sieve. The sample cup is inserted into one of SAM's two pyrolysis ovens, which is first brought to a nominal preheat temperature of ~50 °C for a duration of 6–12 min, then heated to ~850 °C at a rate of 35 °C min^{-1} under 25 mb He pressure. SAM's first oven (oven-1) has an external temperature sensor and the second (oven-2) has a secondary heater wire in lieu of a temperature sensor. Two models have been utilized to date for the estimation of sample temperature in oven-2 experiments: oven-2_model-1 and oven-2_model-2. Data shown in Extended Data Fig. 1 for experiments

using oven-2 were generated with oven-2_model-1, which at present provides the best available estimates of sample temperatures for oven-2. (We note that figures in Sutter et al.⁵ were generated with oven-2_model-2.) Helium carrier gas penetrates the base of the quartz cup, comprising a porous quartz frit, to sweep evolved gases from the oven efficiently. The model-derived He flow rate is 0.8 standard cubic centimetres per minute (sccm). A small portion of the evolved gas is sampled continuously by the QMS throughout the temperature ramp. The QMS scans its entire mass range, from m/z 2 to 535, via a 'smart-scanning' algorithm that optimizes dwell time at masses where signal is detected during each experiment⁴⁷. Evolution peak temperatures for various gases are compared to those of reference materials to constrain parent mineral phases. Integration of the QMS signal over time for a particular m/z value allows quantitative estimation of chemical and isotopic abundances. A portion of the gas stream, parameterized by a desired range of sample temperature, may also be collected during each run for isotopic and abundance analysis of CO₂, H₂O and CH₄ by the TLS or for analysis by the gas chromatograph and QMS.

Extended Data Fig. 2 shows example EGA data obtained with laboratory test stands at Goddard Space Flight Center. The SAM breadboard system includes the prototype QMS for SAM, which is identical to that of the flight model, and a laboratory version of the pyrolysis oven that is easily accessible for loading samples. A second Goddard Space Flight Center test stand includes a Setaram Labsys Evo thermogravimeter/differential scanning calorimeter coupled to a Pfeiffer OmniStar QMS. Both systems are operated under conditions that mimic the performance of the SAM flight model. As seen in Extended Data Fig. 2, continuous monitoring of the gases released as a sample is heated during an EGA experiment provides information helpful in determining the mineral and organic content of the sample. Although this technique cannot conclusively identify specific minerals, EGA is a useful diagnostic tool because volatile-bearing minerals typically release gases at characteristic temperatures, dependent on their composition. For example, under SAM operating conditions, CO₂ released from Fe-carbonate typically peaks at ~600°C, while CO₂ released from Ca-carbonate peaks at ~740°C (Extended Data Fig. 2a). Some carboxylated organic compounds and oxalates release CO₂ at temperatures below this, making them candidate sources for the bulk of CO₂ observed by SAM (Extended Data Fig. 2b–d).

CO₂ isotope ratios. Both carbon and oxygen isotope ratios of CO₂ may be calculated from SAM QMS data. The QMS uses electron-impact ionization and a secondary electron multiplier detector, operated in pulse-counting mode. All data are corrected for detector effects and instrument background as the initial step in quantitative analysis⁴⁷. The QMS is operated primarily in 'unit scan' mode, which counts ions only at integer mass-to-charge ratio m/z values, during SAM EGA experiments⁴⁷. O₂ isotope ratios are computed from isotopologues at m/z 32 and 34, with correction for ¹⁷O contributions to m/z 34. Owing to isobaric interferences from other compounds at m/z 12–13 and 16–18, CO₂ isotope ratios are in principle calculated from isotopologues at m/z 44, 45 and 46. However, because the detector is typically saturated during measurements of m/z 44, the signal for this isotopologue usually must be estimated from the doubly charged ion at m/z 22 using the calibration constant determined during pre-launch testing⁴⁸. In some cases, sufficient data are acquired during the CO₂ peak to allow calculation of isotope ratios using m/z 44 (the RN and JK samples). Unfortunately, low signal at m/z 47 after subtraction of background and correction of isobaric interferences precludes the use of this isotopologue to constrain the CO₂ isotopic composition.

Fragments of MTBSTFA-derived products may produce isobaric interferences with the CO₂ isotopologues used for isotopic analysis. Data were corrected for estimated contributions from the following compounds identified in EGA and gas chromatograph mass spectrometry data, based on mass spectra published by the National Institute of Standards and Technology: 1,3-ditert-butyl-1,1,3,3-tetramethyldisiloxane; tert-butyltrimethylsilanol; tert-butyltrimethylsilyl fluoride; 2,2,2-trifluoroacetamide; 2,2,2-trifluoro-*N*-methylacetamide; trifluoroacetonitrile; and monochlorotrifluoromethane. In most SAM experiments, the combined interferences from these seven compounds affected values of δ¹⁸O and δ¹³C by 2–3‰ or less.

Equations for computing the carbon and oxygen isotope ratios of CO₂, which include corrections for isobaric interferences due to various isotopologues, are given by Franz et al.⁴⁹. A value of 0.32‰ for Δ¹⁷O, representing the average for Martian silicates⁵⁰, is assumed for all calculations. A small correction of 3‰ was applied to values of δ¹⁸O to account for QMS mass fractionation⁴⁹. Results are reported as delta values (δ¹³C and δ¹⁸O), representing per mil deviations from reference standards:

$$\delta^{13}\text{C} = 1,000 \times \left[\left(\frac{^{13}\text{C}/^{12}\text{C}}{(^{13}\text{C}/^{12}\text{C})_{\text{V-PDB}}} - 1 \right) \right] \quad (1)$$

and

$$\delta^{18}\text{O} = 1,000 \times \left[\left(\frac{^{18}\text{O}/^{16}\text{O}}{(^{18}\text{O}/^{16}\text{O})_{\text{V-SMOW}}} - 1 \right) \right] \quad (2)$$

where the reference standard for carbon is V-PDB and that for oxygen is V-SMOW⁵¹.

Isotope ratios are nominally computed from the ratios of integrated areas under the EGA curve in the time domain for the m/z of interest (Supplementary Fig. 4), although the average of ratios of signal at these isotopologues for the same time range yields nearly identical results. Uncertainties in resulting isotope ratios for a given measurement represent the standard error of the mean for m45/est_m44 and m46/est_m44 during the relevant portion of the CO₂ peak.

Supplementary Table 1 also includes isotope data obtained with the TLS for a subset of samples. The sample temperature cut that was directed to the TLS for each sample is noted in column 4. The TLS utilizes a near-infrared tunable laser diode at 2.78 μm to analyse CO₂ and H₂O. Abundances and isotope ratios are calculated by comparison of direct absorption lines with the HITRAN 2012 infrared line list⁵², with minor corrections from calibration gas results using isotopic standards. This enables measurement of δ¹⁸O, δ¹³C and δD^{48,53}.

Data availability

All SAM data are available at NASA's Planetary Data System.

Received: 12 April 2019; Accepted: 28 November 2019;

Published online: 27 January 2020

References

- Freissinet, C. et al. Organic molecules in the Sheepbed mudstone, Gale Crater, Mars. *J. Geophys. Res. Planets* **120**, 495–514 (2015).
- Eigenbrode, J. L. et al. Organic matter preserved in 3-billion-year-old mudstones at Gale crater, Mars. *Science* **360**, 1096–1101 (2018).
- Benner, S. A., Devine, K. G., Matveeva, L. N. & Powell, D. H. The missing organic molecules on Mars. *Proc. Natl Acad. Sci. USA* **97**, 2425–2430 (2000).
- Applin, D. M., Izawa, M. R. M., Cloutis, E. A., Goltz, D. & Johnson, J. R. Oxalate minerals on Mars? *Earth Planet. Sci. Lett.* **420**, 127–139 (2015).
- Sutter, B. et al. Evolved gas analyses of sedimentary rocks and eolian sediment in Gale Crater, Mars: results of the Curiosity rover's Sample Analysis at Mars instrument from Yellowknife Bay to the Namib Dune. *J. Geophys. Res. Planets* **122**, 2574–2609 (2017).
- Pollack, J. B., Kasting, J. F., Richardson, S. M. & Poliakov, K. The case for a warm, wet climate on early Mars. *Icarus* **71**, 203–224 (1987).
- Mahaffy, P. R. et al. Abundance and isotopic composition of gases in the martian atmosphere from the Curiosity rover. *Science* **341**, 263–266 (2013).
- Steele, A. et al. A reduced organic carbon component in martian basalts. *Science* **337**, 212–215 (2012).
- Jakosky, B. M. & Jones, J. H. The history of Martian volatiles. *Rev. Geophys.* **35**, 1–16 (1997).
- Webster, C. R. et al. Isotope ratios of H, C, and O in CO₂ and H₂O of the martian atmosphere. *Science* **341**, 260–263 (2013).
- Jakosky, B. M. et al. Loss of the Martian atmosphere to space: present-day loss rates determined from MAVEN observations and integrated loss through time. *Icarus* **315**, 146–157 (2018).
- Atreya, S. K. et al. Primordial argon isotope fractionation in the atmosphere of Mars measured by the SAM instrument on Curiosity and implications for atmospheric loss. *Geophys. Res. Lett.* **40**, 1–5 (2013).
- Wray, J. J. et al. Orbital evidence for more widespread carbonate-bearing rocks on Mars. *J. Geophys. Res. Planets* **121**, 652–677 (2016).
- Ehlmann, B. L. et al. Orbital identification of carbonate-bearing rocks on Mars. *Science* **322**, 1828–1832 (2008).
- Murchie, S. L. et al. A synthesis of Martian aqueous mineralogy after 1 Mars year of observations from the Mars Reconnaissance Orbiter. *J. Geophys. Res. Planets* **114**, E00D06 (2009).
- Bibring, J. P. et al. Mars surface diversity as revealed by the OMEGA/Mars Express observations. *Science* **307**, 1576–1581 (2005).
- Christensen, P. R. et al. Mars global surveyor thermal emission spectrometer experiment: investigation description and surface science results. *J. Geophys. Res.* **106**, 23823–23871 (2001).
- Pepin, R. O. Evolution of the martian atmosphere. *Icarus* **111**, 289–304 (1994).
- Jakosky, B. M., Pepin, R. O., Johnson, R. E. & Fox, J. L. Mars atmospheric loss and isotopic fractionation by solar-wind-induced sputtering and photochemical escape. *Icarus* **111**, 271–288 (1994).
- Pepin, R. O. On the origin and early evolution of terrestrial planet atmospheres and meteoritic values. *Icarus* **92**, 2–79 (1991).
- Jakosky, B. Mars volatile evolution: evidence from stable isotopes. *Icarus* **94**, 14–31 (1991).
- Luhmann, J. G., Johnson, R. E. & Zhang, M. H. G. Evolutionary impact of sputtering of the martian atmosphere by O⁺ pickup ions. *Geophys. Res. Lett.* **19**, 2151–2154 (1992).
- Lundin, R., Lammer, H. & Ribas, I. Planetary magnetic fields and solar forcing: implications for atmospheric evolution. *Space Sci. Rev.* **129**, 245–278 (2007).

24. Bristow, T. F. et al. Low Hesperian P_{CO_2} constrained from in situ mineralogical analysis at Gale Crater, Mars. *Proc. Natl Acad. Sci. USA* **114**, 2166–2170 (2017).
25. Bultel, B., Viennet, J.-C., Poulet, F., Carter, J. & Werner, S. C. Detection of carbonates in Martian weathering profiles. *J. Geophys. Res. Planets* **124**, 989–1007 (2019).
26. Wright, I. P., Grady, M. M. & Pillinger, C. T. Carbon, oxygen and nitrogen isotopic compositions of possible Martian weathering products in EETA 79001. *Geochim. Cosmochim. Acta* **52**, 917–924 (1988).
27. Halevy, I., Fischer, W. W. & Eiler, J. M. Carbonates in the Martian meteorite Allan Hills 84001 formed at 18 +/- 4 degrees C in a near-surface aqueous environment. *Proc. Natl Acad. Sci. USA* **108**, 16895–16899 (2011).
28. Deines, P. Carbon isotope effects in carbonate systems. *Geochim. Cosmochim. Acta* **68**, 2659–2679 (2004).
29. Craddock, R. A. & Greeley, R. Minimum estimates of the amount and timing of gases released into the martian atmosphere from volcanic eruptions. *Icarus* **204**, 512–526 (2009).
30. Valley, J. W. et al. Low-temperature carbonate concretions in the Martian meteorite ALH84001: evidence from stable isotopes and mineralogy. *Science* **275**, 1633–1638 (1997).
31. Chacko, T. & Deines, P. Theoretical calculation of oxygen isotope fractionation factors in carbonate systems. *Geochim. Cosmochim. Acta* **72**, 3642–3660 (2008).
32. Toyota, T. et al. Oxygen isotope fractionation during the freezing of sea water. *J. Glaciol.* **59**, 697–710 (2013).
33. Staudigel, P. T. et al. Cryogenic brines as diagenetic fluids: reconstructing the diagenetic history of the Victoria Land Basin using clumped isotopes. *Geochim. Cosmochim. Acta* **224**, 154–170 (2018).
34. Fairen, A. G. et al. A cold hydrological system in Gale crater, Mars. *Planet. Space Sci.* **93–94**, 101–118 (2014).
35. Friedman, I. & O'Neil, J. R. in *Data of Geochemistry* 6th edn (ed. M. Fleischer) Ch. KK (USGS, 1977).
36. Elsila, J. E., Charnley, S. B., Burton, A. S., Glavin, D. P. & Dworkin, J. P. Compound-specific carbon, nitrogen, and hydrogen isotopic ratios for amino acids in CM and CR chondrites and their use in evaluating potential formation pathways. *Meteorit. Planet. Sci.* **47**, 1517–1536 (2012).
37. Stern, J. C. et al. The nitrate/(per)chlorate relationship on Mars. *Geophys. Res. Lett.* **44**, 2643–2651 (2017).
38. Lasne, J. et al. Oxidants at the surface of Mars: a review in light of recent exploration results. *Astrobiology* **16**, 977–996 (2016).
39. Davidson, J. A. et al. Carbon kinetic isotope effect in the reaction of CH_4 with HO . *J. Geophys. Res. Atmos.* **92**, 2195–2199 (1987).
40. Rudolph, J., Czuba, E. & Huang, L. The stable carbon isotopic fractionation for reactions of selected hydrocarbons with OH-radicals and its relevance for atmospheric chemistry. *J. Geophys. Res.* **105**, 29329–29346 (2000).
41. Atreya, S. K. & Gu, Z. G. Photochemistry and stability of the atmosphere of Mars. *Adv. Space Res.* **16**, 657–658 (1995).
42. Hori, Y., Murata, A. & Yoshinami, Y. Adsorption of CO , intermediately formed in electrochemical reduction of CO_2 , at a copper electrode. *J. Chem. Soc. Faraday Trans.* **87**, 125 (1991).
43. Rahn, T. & Eiler, J. M. Experimental constraints on the fractionation of $^{13}\text{C}/^{12}\text{C}$ and $^{18}\text{O}/^{16}\text{O}$ ratios due to adsorption of CO_2 on mineral substrates at conditions relevant to the surface of Mars. *Geochim. Cosmochim. Acta* **65**, 839–846 (2001).
44. Bridges, J. C., Hicks, L. J. & Treiman, A. H. in *Volatiles in the Martian Crust* (eds J. Filiberto & S. P. Schwenzer) 89–118 (Elsevier, 2019).
45. Franz, H. B. et al. Large sulfur isotope fractionations in Martian sediments at Gale crater. *Nature Geosci.* **10**, 658–662 (2017).
46. Webster, C. R. et al. Background levels of methane in Mars' atmosphere show strong seasonal variations. *Science* **360**, 1093–1096 (2018).
47. Franz, H. B. et al. Analytical techniques for retrieval of atmospheric composition with the quadrupole mass spectrometer of the Sample Analysis at Mars instrument suite on Mars Science Laboratory. *Planet. Space Sci.* **96**, 99–113 (2014).
48. Franz, H. B. et al. Reevaluated martian atmospheric mixing ratios from the mass spectrometer on the Curiosity rover. *Planet. Space Sci.* **109–110**, 154–158 (2015).
49. Franz, H. B. et al. Initial SAM calibration gas experiments on Mars: quadrupole mass spectrometer results and implications. *Planet. Space Sci.* **138**, 44–54 (2017).
50. Franchi, I. A., Wright, I. P., Sexton, A. S. & Pillinger, C. T. The oxygen-isotopic composition of Earth and Mars. *Meteorit. Planet. Sci.* **34**, 657–661 (1999).
51. Coplen, T. B. New IUPAC guidelines for the reporting of stable hydrogen, carbon, and oxygen isotope-ratio data. *J. Res. Natl Inst. Stand. Technol.* **100**, 285 (1995).
52. Rothman, L. S. et al. The HITRAN2012 molecular spectroscopic database. *J. Quant. Spectrosc. Radiat. Trans.* **130**, 4–50 (2013).
53. Mahaffy, P. R. et al. The imprint of atmospheric evolution in the D/H of Hesperian clay minerals on Mars. *Science* **347**, 412–414 (2015).

Acknowledgements

This work was funded by NASA's Mars Exploration Program. We thank T. B. Griswold for figure production, R. H. Becker for discussion, and the technical team at the NASA Goddard Space Flight Center Planetary Environments Laboratory for laboratory support.

Author contributions

H.B.F. developed QMS analytical methods, calculated QMS isotope ratios, interpreted results, performed calibration experiments, and wrote the manuscript and the Supplementary Information. C.R.W. and G.L.F. developed TLS analytical methods and calculated TLS isotope ratios. E.R., C.F. and M.M. assisted with QMS data analysis. H.B.F., A.C.McA., C.A.K., P.D.A. and J.M.T.L. performed supporting laboratory experiments. J.C.S. performed ground-truth isotopic analyses of calibrants. All authors participated in discussion of results or editing of the manuscript.

Competing interests

The authors declare no competing interests

Additional information

Extended data is available for this paper at <https://doi.org/10.1038/s41550-019-0990-x>.

Supplementary information is available for this paper at <https://doi.org/10.1038/s41550-019-0990-x>.

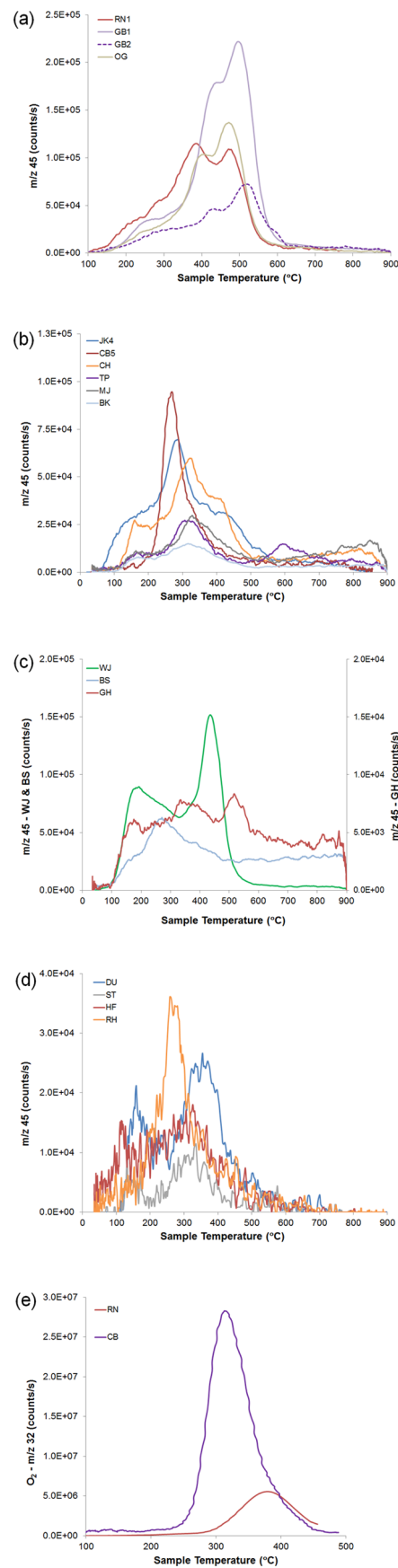
Correspondence and requests for materials should be addressed to H.B.F.

Peer review information *Nature Astronomy* thanks Alberto Fairen and the other, anonymous, reviewer(s) for their contribution to the peer review of this work.

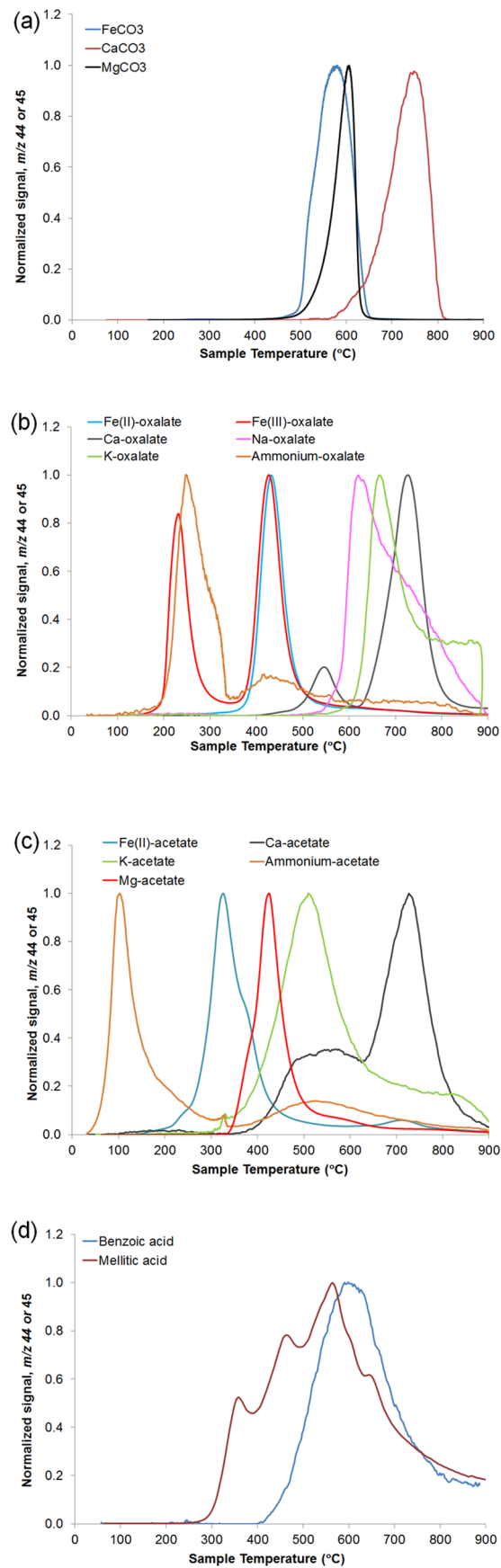
Reprints and permissions information is available at www.nature.com/reprints.

Publisher's note Springer Nature remains neutral with regard to jurisdictional claims in published maps and institutional affiliations.

This is a U.S. government work and not under copyright protection in the U.S.; foreign copyright protection may apply 2020



Extended Data Fig. 1 | CO_2 and O_2 evolved from Gale crater samples. CO_2 (isotopologue at m/z 45) evolved from aeolian (a), mudstone (except Vera Rubin Ridge) (b), sandstone (c) and Vera Rubin Ridge samples (d). e, O_2 evolved from RN and CB samples. Data for samples in panels a–c have been normalized to a single portion aliquot.



Extended Data Fig. 2 | Laboratory CO_2 data. CO_2 profile (isotopologue at m/z 44 or 45) from EGA analyses with laboratory test stands: carbonates (a); oxalates (b); acetates (c); benzoic and mellitic acids (d). The peak temperatures of CO_2 evolved from Martian samples by SAM are compared with those from laboratory runs such as these to help identify the mineral phases present. The CaCO_3 was the same synthetic material used for SAM flight model calibration.

Terms and Conditions

Springer Nature journal content, brought to you courtesy of Springer Nature Customer Service Center GmbH (“Springer Nature”).

Springer Nature supports a reasonable amount of sharing of research papers by authors, subscribers and authorised users (“Users”), for small-scale personal, non-commercial use provided that all copyright, trade and service marks and other proprietary notices are maintained. By accessing, sharing, receiving or otherwise using the Springer Nature journal content you agree to these terms of use (“Terms”). For these purposes, Springer Nature considers academic use (by researchers and students) to be non-commercial.

These Terms are supplementary and will apply in addition to any applicable website terms and conditions, a relevant site licence or a personal subscription. These Terms will prevail over any conflict or ambiguity with regards to the relevant terms, a site licence or a personal subscription (to the extent of the conflict or ambiguity only). For Creative Commons-licensed articles, the terms of the Creative Commons license used will apply.

We collect and use personal data to provide access to the Springer Nature journal content. We may also use these personal data internally within ResearchGate and Springer Nature and as agreed share it, in an anonymised way, for purposes of tracking, analysis and reporting. We will not otherwise disclose your personal data outside the ResearchGate or the Springer Nature group of companies unless we have your permission as detailed in the Privacy Policy.

While Users may use the Springer Nature journal content for small scale, personal non-commercial use, it is important to note that Users may not:

1. use such content for the purpose of providing other users with access on a regular or large scale basis or as a means to circumvent access control;
2. use such content where to do so would be considered a criminal or statutory offence in any jurisdiction, or gives rise to civil liability, or is otherwise unlawful;
3. falsely or misleadingly imply or suggest endorsement, approval, sponsorship, or association unless explicitly agreed to by Springer Nature in writing;
4. use bots or other automated methods to access the content or redirect messages
5. override any security feature or exclusionary protocol; or
6. share the content in order to create substitute for Springer Nature products or services or a systematic database of Springer Nature journal content.

In line with the restriction against commercial use, Springer Nature does not permit the creation of a product or service that creates revenue, royalties, rent or income from our content or its inclusion as part of a paid for service or for other commercial gain. Springer Nature journal content cannot be used for inter-library loans and librarians may not upload Springer Nature journal content on a large scale into their, or any other, institutional repository.

These terms of use are reviewed regularly and may be amended at any time. Springer Nature is not obligated to publish any information or content on this website and may remove it or features or functionality at our sole discretion, at any time with or without notice. Springer Nature may revoke this licence to you at any time and remove access to any copies of the Springer Nature journal content which have been saved.

To the fullest extent permitted by law, Springer Nature makes no warranties, representations or guarantees to Users, either express or implied with respect to the Springer nature journal content and all parties disclaim and waive any implied warranties or warranties imposed by law, including merchantability or fitness for any particular purpose.

Please note that these rights do not automatically extend to content, data or other material published by Springer Nature that may be licensed from third parties.

If you would like to use or distribute our Springer Nature journal content to a wider audience or on a regular basis or in any other manner not expressly permitted by these Terms, please contact Springer Nature at

onlineservice@springernature.com